Acid Efflux from Retinal Glial Cells Generated by Sodium Bicarbonate Cotransport

Eric A. Newman

Department of Physiology, University of Minnesota, Minneapolis, Minnesota 55455

Sodium bicarbonate cotransport was studied in freshly dissociated Müller cells of the salamander retina. Variations in intracellular and extracellular pH evoked by elevating extracellular potassium concentration ($[K^+]_o$) were recorded. Intracellular pH was measured by standard ratio imaging of the pH-sensitive dye BCECF, whereas extracellular pH was monitored by imaging BCECF fixed to coverslips under dissociated cells. Increasing $[K^+]_o$ from 2.5 to 50 mM resulted in an intracellular alkalinization. The rate of alkalinization, 0.047 pH units/min, was reduced to 42% of control when HEPES was substituted for HCO_3^- and was reduced to 36% of control by the addition of 0.5 mM DIDS, a Na^+/HCO_3^- cotransport blocker. The K^+-evoked alkalinization was Cl^--independent and was not substantially reduced by amiloride or bumetanide. Increasing $[K^+]_o$ to 50 mM also produced a rapid extracellular acidification, 0.01 to 0.05 pH units in amplitude. HEPES substitution and addition of 0.5 mM DIDS reduced the acidification to 7–8% of control, respectively. These results confirm the presence of a Na^+/HCO_3^- cotransport system in salamander Müller cells and provide definitive evidence that glial cells can generate an extracellular acidification when $[K^+]_o$ is increased.

The K^+-evoked extracellular acidification measured beneath cell endfeet was 304% of the amplitude of the acidification beneath cell somata, confirming that cotransporter sites are preferentially localized to the endfoot. The carbonic anhydrase inhibitor benzolamide (2×10^{-5} M), which is poorly membrane permeant, increased the K^+-evoked extracellular acidification to 269% of control, demonstrating that salamander Müller cells possess extracellular carbonic anhydrase.

Key words: glial cell; Müller cell; retina; Na^+/HCO_3^- cotransport; pH; BCECF; salamander

Neuronal activity in the central nervous system (CNS) typically results in a transient alkalinization of extracellular space followed by a sustained acidification (Chesler, 1990; Chesler and Kaila, 1992). The transient alkalinization is associated with synaptic activity and is generated by the activation of both glutamatergic and GABAergic receptors (Jarolimek et al., 1989; Chen and Chesler, 1992b; Kaila et al., 1992). In contrast, the sustained acidification can be generated in the absence of synaptic activation (Ransom et al., 1988) and may be caused by acid efflux (Sykova and Svoboda, 1990) as well as by the release of CO_2 (Voipio and Kaila, 1993) from activated neurons.

These activity-dependent variations in extracellular pH (pH_o) may significantly influence neuronal activity (Balestrino and Somjen, 1988; Taira et al., 1993; Gottfried and Chesler, 1994). For example, pH_o modulates synaptic transmission (Balestrino and Somjen, 1988; Jarolimek et al., 1989; Taira et al., 1993; Gottfried and Chesler, 1994). NMDA receptor conductance is strongly dependent on pH_o, with proton concentration modulating the kinetics of channel gating (Tang et al., 1990; Traynelis and Cull-Candy, 1990). Similarly, protons block voltage-dependent Ca^{2+} channels (Prod'hom et al., 1987; Krafte and Kass, 1988; Barnes and Bui, 1991; Klockner and Isenberg, 1994) and modulate synaptic transmission by reducing Ca^{2+} influx at presynaptic terminals (Barnes et al., 1993). A dramatic example of pH_o modulation of synaptic efficacy is provided by the retina, in which synaptic transmission between photoreceptors and second-order cells is reduced substantially by extracellular acidification (Harsanyi and Mangel, 1993; Kleinschmidt, 1994); in one preparation by 24% when pH_o is reduced by just 0.05 pH units (Barnes et al., 1993).

Glial cells in the CNS may contribute to the extracellular acidification initiated by neuronal activity. Several types of glial cells possess an electrogenic Na^+/HCO_3^- cotransport system (Astion and Orkand, 1988; Kettenmann and Schlue, 1988; Newman, 1991; O'Connor et al., 1994). The activity of the cotransporter is modulated by changes in cell membrane potential (Boron and Boulpaep, 1983, 1989). Neuronal activity increases extracellular potassium concentration ($[K^+]_o$), which depolarizes glial cells and intensifies the transport of Na^+ and HCO_3^- into glial cells. The increased influx of HCO_3^- produces a cell alkalinization and may acidify extracellular space.

The present study was undertaken to provide a direct test of whether glial cells, when stimulated by an increase in $[K^+]_o$, generate transmembrane acid/base fluxes and acidify extracellular space. Freshly dissociated Müller cells, the principal glial cells of the vertebrate retina, were used to determine the effect of glia on pH_o in the absence of neurons. Both intracellular and extracellular pH was monitored as $[K^+]_o$ was increased. Intracellular pH (pH_i) was measured using standard BCECF ratio imaging techniques, whereas pH_o was monitored using a novel method in which BCECF was fixed to coverslips beneath cells. The results confirm that glial cells do indeed acidify extracellular space when stimulated by elevated $[K^+]_o$.

MATERIALS AND METHODS

Cell dissociation. Müller cells of the tiger salamander (*Ambystoma tigrinum*, aquatic stage) were used. Animals were killed by decapitation and pithing. Cells were dissociated as described previously (Newman, 1985).

Received June 12, 1995; revised Sept. 5, 1995; accepted Sept. 20, 1995.

This work was supported by NIH Grant EY-04077. I thank Vincent A. Barnett for his assistance in measuring the excitation and emission spectra of dextran-BCECF and Janice I. Gepner and Kathleen R. Zahs for their helpful comments on the manuscript.

Correspondence should be addressed to Dr. Eric A. Newman, 6-255 Millard Hall, Department of Physiology, University of Minnesota, 435 Delaware Street SE, Minneapolis, MN 55455.

Briefly, isolated retinae were incubated in Ca^{2+}-, Mg^{2+}-free Ringer's containing papain (20 U/3 ml) and cysteine (2 mM). The tissue was rinsed and maintained on ice in HCO_3^- Ringer's containing 1% bovine serum albumin and 0.1% DNase for a period of 3–8 hr. Cells were isolated by triturating the tissue with a series of Pasteur pipettes with progressively smaller tip openings. Dissociated cells were placed in a perfusion chamber and settled onto a glass coverslip coated with either concanavalin A (Con A) or dextran-BCECF and Con A (see below). The chamber was perfused with a gravity-fed system having an exchange time of ~13 sec (80% replacement; Newman, 1994). Gas-impermeant Saran tubing was used throughout.

pH imaging. pH was measured by excitation ratio imaging of the pH-sensitive fluorescent dye BCECF, as described previously (Newman, 1994). BCECF was excited at two wavelengths, and the ratio of the fluorescence emission was computed using the image processing program Image-1 (Universal Imaging, West Chester, PA). Background images were subtracted before computing ratio images. Dissociated cells were imaged using an inverted microscope with a 40×, 0.95 NA objective and an intensified CCD camera (KS-1381, Videoscope International, Washington, DC).

Intracellular pH. For measurements of pH_i, dissociated Müller cells were filled with BCECF using the membrane-permeant form of the dye, BCECF-AM. Dissociated cells were incubated in 16 μM BCECF-AM in HCO_3^- Ringer's for 16 min at 0°C and then rinsed in HCO_3^- Ringer's. The dye was excited at 490 nm and at 440 nm (the isosbestic excitation wavelength), and fluorescence emission was monitored at 535 nm (filter set XF16, Omega Optical, Brattleboro, VT). After completion of an experiment, pH_i for each cell was calibrated by perfusing with a high K^+-nigericin solution at pH 7.0. Emission ratios (490 nm excitation divided by 440 nm excitation) were converted to pH values using this single-point calibration and a modified Michaelis–Menten calibration equation described previously (Newman, 1994),

$$\frac{I_{490}}{I_{440}} = 1 + b \times \left(\frac{10^{(\mathrm{pH}-pK)}}{1 + 10^{(\mathrm{pH}-pK)}} - \frac{10^{(7.0-pK)}}{1 + 10^{(7.0-pK)}} \right), \quad (1)$$

where I_{490}/I_{440} represents the fluorescence emission ratio, normalized to the ratio at pH 7.0. The two parameters in Equation 1 describing the pH sensitivity of BCECF, pK and b, equal 7.25 and 1.82, respectively, as determined previously (Newman, 1994).

Extracellular pH. A variant of the standard ratio imaging technique was developed to measure pH_o immediately outside of dissociated cells. The coverslips under the isolated cells were coated with a thin layer of BCECF before use. Ratio imaging of this extracellular BCECF yielded a measure of pH, both of the bath solution and of the solution in the narrow space between the dissociated cells and the underlying coverslip.

Coverslips were coated with BCECF using the following protocol. Coverslips were cleaned in 100% ethanol, rinsed in H_2O, coated with gelatin (1% aqueous solution), and air-dried. A 1% solution of dextran-conjugated BCECF (70,000 MW) in HEPES Ringer's was then applied to the coverslips, with 2 μl of the solution covering an area of 0.4 cm^2 added to each coverslip. The coverslips were air-dried and fixed overnight in formaldehyde fumes at 36°C, postfixed in 4% formaldehyde for 30 min, rinsed five times in H_2O, and air-dried. A Con A solution was applied to the coverslips over the dextran-BCECF (100 μl of 0.15% Con A in H_2O, covering ~1.3 cm^2 per coverslip) and air-dried.

The fluorescence properties of dextran-BCECF fixed with formaldehyde were characterized with fluorescence spectroscopy. Excitation spectra (Fig. 1*A*) show that an excitation wavelength of 508 nm produces maximal emission, whereas the isosbestic wavelength is 465 nm (for pH values 6.6–8.2). Emission for the dye peaks at 536 nm (Fig. 1*B*). pH_o measurements using dextran-BCECF were made with excitation filters 465 nm (20 nm bandpass) and 508 nm (10 nm bandpass), and emission was monitored at 535 nm (25 nm bandpass). Emission ratios were calculated (508 nm excitation divided by 465 nm excitation) after subtraction of background images. Changes in pH_o were small (0.01–0.05 pH units), and signals were averaged for 5–15 sec to reduce noise. This limited the temporal resolution of pH_o measurements to ~10 sec.

The pH sensitivity of formaldehyde-fixed dextran-BCECF was determined in calibration experiments. Coverslips were perfused in a series of HEPES Ringer's with pH values ranging from 6.2 to 8.2. As the pH increased, the BCECF emission ratio rose in a sigmoidal fashion, in a manner similar to that observed for pH_i measurements. Calibration curves were fit with a modified Equation 1, with ratio values normalized to pH 7.4 instead of 7.0. Mean values for equation parameters pK and b were equal to 6.87 ± 0.08 and 0.712 ± 0.019 (n = 8), respectively.

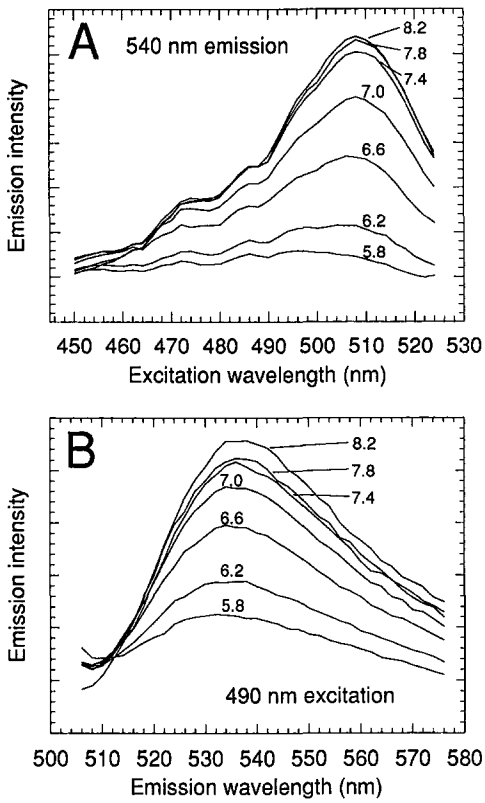

Figure 1. Excitation and emission spectra of dextran-BCECF fixed to coverslips with formaldehyde. BCECF-coated coverslips were bathed in HEPES Ringer's with pH values indicated. *A*, Excitation spectra. Fluorescence emission measured at 540 nm. Peak emission occurs for an excitation wavelength of 508 nm. For pH values 6.6–8.2, the isosbestic wavelength is 465 nm. *B*, Emission spectra. BCECF excited at 490 nm. Peak emission occurs at 536 nm.

In addition to using standard ratio imaging techniques to measure pH_o, pH changes were determined by calculating "difference ratio images." Fluorescence images of BCECF bound to coverslips were obtained using 508 nm excitation (the pH-sensitive wavelength), averaging 256 consecutive frames. Images were obtained during a test period and during control periods before and after the test period. After background subtraction, a difference ratio image was calculated by dividing the average of the two control images by the test image. Changes in BCECF fluorescence, which reflect shifts in pH_o, were typically <1%, and low pass spatial averaging was used to reduce noise. Images were calibrated by converting percentage change in fluorescence to pH_o changes using the calibration equation described above and assuming an initial pH_o of 7.4. Averaged images were acquired with 16-bit resolution, and difference ratio images were computed using Metamorph software (Universal Imaging).

Solutions. HCO_3^--buffered Ringer's contained (in mM): NaCl 80.0, KCl 2.5, $CaCl_2$ 1.8, $MgCl_2$ 0.8, dextrose 10.0, and $NaHCO_3$ 26. It was equilibrated with 5% CO_2 in O_2 and had a pH of ~7.4 at room temperature. HEPES-buffered Ringer's contained (in mM): NaCl 98.5, KCl 2.5, $CaCl_2$ 1.8, $MgCl_2$ 0.8, dextrose 10.0, and HEPES 10.0. It was adjusted to pH 7.4 with NaOH and equilibrated with 100% O_2. In high K^+ solutions, KCl was substituted for NaCl. In zero Na^+ solutions, *N*-methyl-D-glucamine chloride was substituted for NaCl, and choline bicarbonate for $NaHCO_3$. In zero Cl^- solutions, methane sulfonate was substituted for Cl^-. The high K^+-nigericin calibration solution contained *N*-methyl-D-glucamine, 18.5 mM; KCl, 72.5 mM; $CaCl_2$, 1.8 mM; $MgCl_2$, 0.8 mM; dextrose, 10.0 mM; HEPES, 20.0 mM; and nigericin, 10 μM.

Dextran-BCECF (70,000 MW), BCECF-AM, and nigericin were obtained from Molecular Probes (Eugene, OR); amiloride, bumetanide, and methazolamide were obtained from Sigma (St. Louis, MO). Benzo-

lamide was the generous gift of Thomas Maren and Curtis Conroy. Results are given as mean ± SD (n).

RESULTS

Resting intracellular pH

The resting pH_i of dissociated Müller cells was determined in HCO_3^- and HEPES Ringer's. In HCO_3^--buffered Ringer's, pH_i equaled 7.08 ± 0.04 (27), whereas in HEPES, pH_i equaled 6.96 ± 0.06 (44). When the bathing solution was switched from HCO_3^- to HEPES, pH_i, responding to a decrease in P_{CO_2}, transiently shifted to a more alkaline value before gradually acidifying over a 20–35 min period. The shift to a more acidic resting pH_i indicates that one or more HCO_3^- transport systems contribute to pH_i regulation in Müller cells.

There was little change in pH_i when Cl^- was removed from the bathing solution, suggesting that Cl^--dependent transporters are not involved in maintaining steady state pH_i. In HCO_3^--buffered solution, removal of Cl^- reduced pH_i by only 0.03 pH units, to 7.05 ± 0.03 (10). In HEPES-buffered solution, pH_i, in the absence of Cl^-, was 6.96 ± 0.04 (8), identical to the value measured with Cl^- present.

K^+-induced intracellular alkalinization

Many glial cells (Astion and Orkand, 1988; Kettenmann and Schlue, 1988; O'Connor et al., 1994), including Müller cells (Newman, 1991), possess a Na^+/HCO_3^- cotransport system. The cotransporter is electrogenic, transporting one Na^+ along with two or three HCO_3^-. Depending on the precise stoichiometry, which varies in different preparations (Soleimani et al., 1987; Deitmer and Schlue, 1989; Hughes et al., 1989; Newman, 1991; O'Connor et al., 1994), the reversal potential of the cotransporter is somewhat positive or negative of the cell membrane potential. When the cell resting potential is positive to the cotransporter reversal potential, Na^+ and HCO_3^- are tonically transported into the cell. When the cell is depolarized, this Na^+ and HCO_3^- influx is increased.

Cotransporter activity can be assessed by monitoring pH_i as $[K^+]_o$ is varied. Raising $[K^+]_o$ depolarizes cells and should lead to an intracellular alkalinization, generated by the increased influx of HCO_3^- through the cotransporter.

In the current study, increasing $[K^+]_o$ did indeed produce an intracellular alkalinization in Müller cells (Fig. 2). In response to a step increase in $[K^+]_o$, intracellular alkalinization proceeded at a near constant rate for several minutes, slowing down and eventually reaching plateau after 10 min or more. When $[K^+]_o$ was subsequently reduced to the control level of 2.5 mM, pH_i recovered to near baseline pH_i. The initial rate of alkalinization, rather than the final, plateau value of pH_i, was measured to quantify the response, as it gives a more accurate measure of Na^+/HCO_3^- cotransport activity.

In some cells, the K^+-evoked alkalinization proceeded in two phases: an initial, rapid alkalinization lasting 10–20 sec, followed by a slower alkalinization continuing for several minutes. The initial rapid phase of alkalinization was quite distinct in some cells (*arrows* in Figs. 2*B* and 4); its origin is not known. It is probably not caused by K^+-induced cell swelling, however, which would lead to a $[HCO_3^-]_i$ decrease and to an intracellular acidification.

The rate of K^+-induced intracellular alkalinization was quantified by fitting a tangent line by eye to pH_i records. The initial, rapid phase of alkalinization was disregarded when making these measurements. The K^+-induced alkalinization rate was equal to 0.047 ± 0.013 (39) pH units/min when $[K^+]_o$ was increased from 2.5 to 50 mM. (The average rate of K^+-induced alkalinization varied somewhat in different groups of animals and times of year. The reason for this variation is not known.)

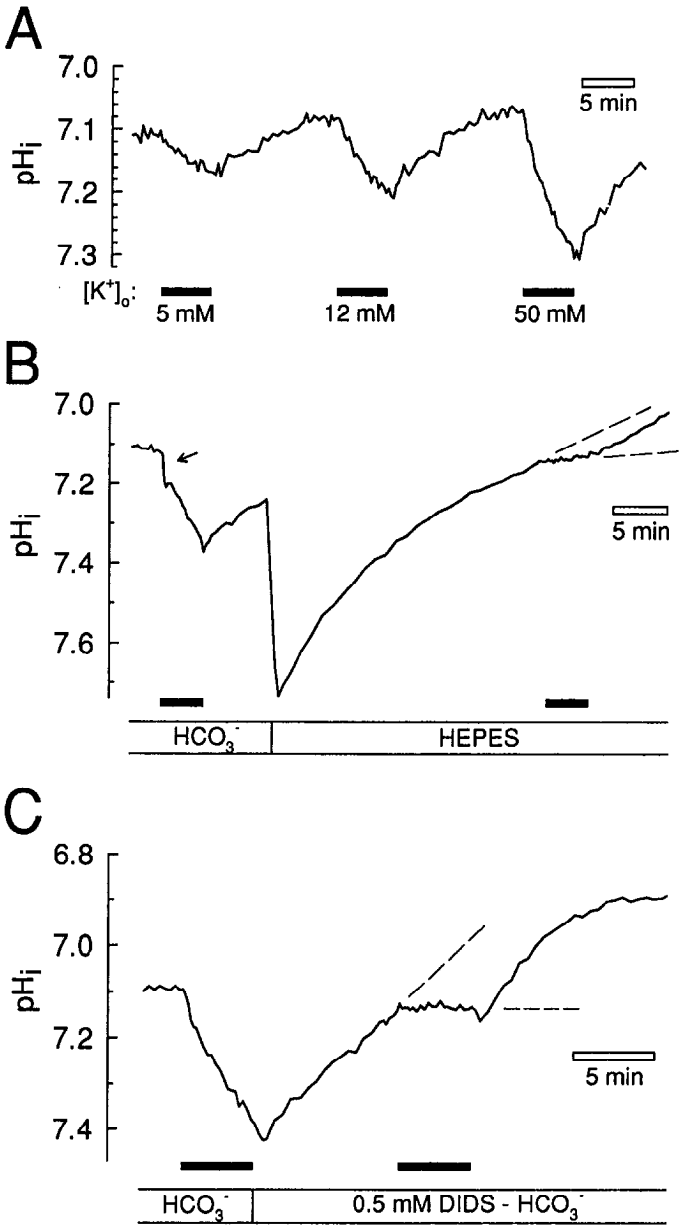

Figure 2. Potassium-evoked intracellular alkalinization in salamander Müller cells. *A*, The rate and extent of alkalinization is greater for larger increases in $[K^+]_o$. Application of high $[K^+]_o$ solutions are indicated by *filled bars*. Note that acidification (an increase in $[H^+]$) is indicated as an upward deflection in this and subsequent pH plots. *B*, Substitution of HEPES for HCO_3^- reduces the rate of K^+-evoked intracellular alkalinization. HEPES substitution generates a transient alkalinization followed by a slow acidification and results in the reduction of the K^+-evoked alkalinization, in this example, to 50% of control. The alkalinization rate in HEPES is measured as the difference between the slope of the plot during high K^+ application and the slope just before application (indicated by *dashed lines*). In this and the following figures, application of 50 mM $[K^+]_o$ solutions is indicated by *filled bars* below the plots. *Arrow* indicates initial rapid phase of K^+-evoked alkalinization (see text). *C*, Addition of 0.5 mM DIDS, a Na^+/HCO_3^- cotransport blocker, reduces the rate of K^+-evoked alkalinization, in this example, to 43% of control. Note that DIDS addition results in an acidification of the resting pH_i.

The relation between the rate of alkalinization and the magnitude of the $[K^+]_o$ increase was determined in individual cells by

exposing them sequentially to 5, 12, and 50 mM $[K^+]_o$ (Fig. 2*A*). Mean alkalinization rates were 0.008 ± 0.004, 0.017 ± 0.005, and 0.035 ± 0.011 (8) pH units/min, respectively, for the three $[K^+]_o$ levels.

Na^+/HCO_3^- cotransport

The K^+-induced alkalinization described above could be generated by the voltage-dependent Na^+/HCO_3^- cotransport system of Müller cells. If this cotransporter were solely responsible for the alkalinization, the K^+-induced pH shift would be abolished by removal of HCO_3^- from the bathing solution and by addition of cotransporter blockers. This proved to be only partially true.

Cell alkalinization evoked by raising $[K^+]_o$ was reduced, but not eliminated, when the bath solution was switched from HCO_3^--buffered to HEPES-buffered Ringer's (Fig. 2*B*). To obtain an accurate comparison of the K^+-induced alkalinizations in HCO_3^- and HEPES Ringer's, the two responses were measured at the same pH_i. This avoided the potential complication of the HCO_3^--independent component of the alkalinization being pH-dependent. Replacement of HCO_3^- with HEPES resulted in an initial alkalinization followed by a slow acidification (Fig. 2*B*), which eventually reached plateau at a pH more acidic than the resting pH in HCO_3^-. The K^+-evoked alkalinization in HEPES was measured at the time when the acidifying pH_i crossed the control pH_i level. Typically, K^+ application did not produce an actual alkalinization, but rather produced a reduction in the rate of acidification. The rate of K^+-evoked "alkalinization" in HEPES was calculated as the difference in the pH_i slope at times just before and during K^+ application (Fig. 2*B*, *dashed lines*).

Cell alkalinization evoked by raising $[K^+]_o$ from 2.5 to 50 mM was reduced from 0.046 ± 0.008 to 0.019 ± 0.008 (16) pH units/min when the bath solution was switched from HCO_3^--buffered to HEPES-buffered Ringer's, a reduction to 42% of the control response. Intracellular buffering power is substantially lower for cells bathed in HEPES Ringer's compared with cells in HCO_3^- Ringer's (Chesler, 1990). Thus, the HCO_3^--independent component of the alkalinization observed in HEPES is larger than it would be if the CO_2/HCO_3^- buffering system were present.

Addition of the cotransport inhibitor 4,4′-diisothiocyanato-stilbene-2,2′-disulfonic acid (DIDS; Boron and Boulpaep, 1989) had an effect on the K^+-induced alkalinization similar to that of HCO_3^- removal. Raising $[K^+]_o$ to 50 mM produced an alkalinization that was reduced from 0.045 ± 0.009 to 0.017 ± 0.007 (12) pH units/min on addition of 0.5 mM DIDS, a reduction to 36% of the control response (Fig. 2*C*). As in the HEPES-substitution experiment, the K^+-induced alkalinization in DIDS was measured at the time when the acidifying pH_i equaled the control baseline.

Steady-state pH_i shifted from 7.11 ± 0.01 to 6.86 ± 0.14 (9) on addition of DIDS. This DIDS-evoked acidification provides additional support for the supposition that HCO_3^--dependent transport systems play a role in establishing resting pH_i.

If the K^+-evoked alkalinization is generated by the Na^+/HCO_3^- cotransporter, in addition to being HCO_3^--dependent and DIDS-sensitive, it also should be Na^+-dependent. When Na^+ was removed from the HCO_3^- bath, pH_i acidified steadily and relatively rapidly (Fig. 3*A*). The rate of acidification was equal to 0.079 ± 0.014 (7) pH units/min. The speed of the acidification made it impractical to measure the Na^+-dependency of the K^+-induced alkalinization at control pH_i levels, and its dependency on Na^+ was not determined. The acidification evoked by Na^+ removal is consistent, however, with the presence of a Na^+/HCO_3^- cotransporter in Müller cells.

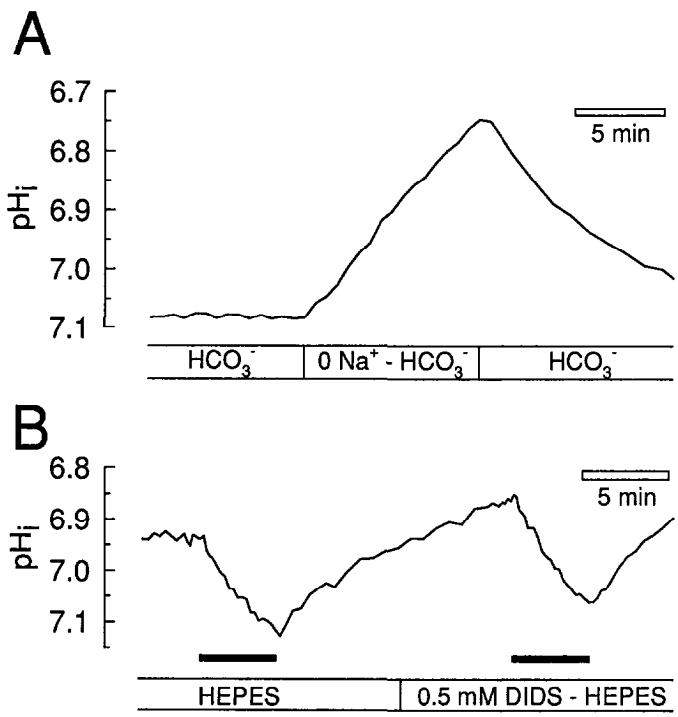

Figure 3. *A*, Removal of Na^+ results in a rapid intracellular acidification. *N*-methyl-D-glucamine and choline are substituted for Na^+ in the HCO_3^- solution. *B*, DIDS has no effect on the HCO_3^--independent component of intracellular alkalinization. The rate of K^+-evoked alkalinization in HEPES Ringer's is not substantially altered by the addition of 0.5 mM DIDS.

The observation that HCO_3^- removal and DIDS addition reduce the K^+-evoked alkalinization to 42 and 36%, respectively, of the control responses supports the conjecture that a large fraction (but not all) of the alkalinization is generated by modulation of a Na^+/HCO_3^- cotransport system. The nature of the HCO_3^--independent component of the K^+-evoked alkalinization remains unclear.

It is possible that a Cl^--dependent transporter contributes to the K^+-evoked alkalinization. This proved not to be the case. Dissociated cells were bathed in Cl^--free Ringer's for periods ranging from 37 to 65 min before testing for depolarization-induced alkalinization. In the absence of Cl^-, the rate of alkalinization evoked by raising $[K^+]_o$ to 50 mM equaled 0.047 ± 0.009 (10) pH units/min, a rate identical to that with Cl^- present.

Similarly, the alkalinization was not substantially diminished by blockers of other transport systems. In the presence of 2 mM amiloride, a blocker of Na^+/H^+ exchange, the rate of alkalinization was 81.9 ± 7.2% (5) of control. With the addition of 20 μM bumetanide, a blocker of $Na^+/K^+/2Cl^-$ cotransport, the rate of alkalinization was 86.5 ± 6.3% (3) of control.

HCO_3^--independent intracellular alkalinization

If the alkalinization that occurs in the absence of HCO_3^- is truly independent of the Na^+/HCO_3^- cotransport system, this component of the K^+-evoked response should not be blocked by DIDS. This proved to be the case (Fig. 3*B*). The rate of K^+-evoked alkalinization in a group of cells bathed in HEPES solution was 0.022 ± 0.009 (17) pH units/min and was essentially unchanged (101 ± 22% of control) after addition of 0.5 mM DIDS.

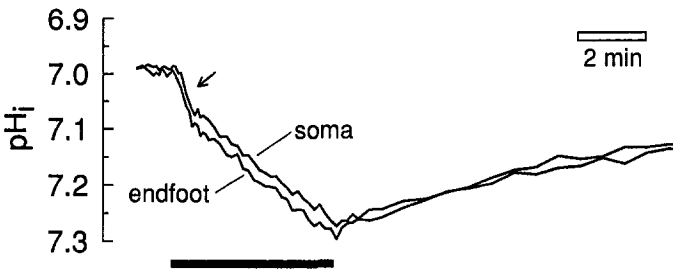

Figure 4. The rate of K^+-evoked alkalinization is identical in all cell regions. The intracellular alkalinization is recorded simultaneously from the *endfoot* and *soma* of a single cell. The rate of alkalinization is the same in both cell regions. The slight offset in the two pH_i records is because of a larger initial rapid phase of the alkalinization (indicated by *arrow*) in the endfoot record.

Carbonic anhydrase

Müller cells have high levels of intracellular carbonic anhydrase (CA). If a large fraction of the K^+-evoked alkalinization is generated by a transmembrane HCO_3^- flux, CA might be expected to influence the alkalinization. This was tested by determining the effect of methazolamide, which inhibits CA in Müller cells (Newman, 1994), on the rate of K^+-evoked alkalinization.

The K^+-induced response was unchanged on addition of 10^{-4} M methazolamide. The rate of alkalinization in a group of cells bathed in HCO_3^- solution was 0.036 ± 0.010 (12) pH units/min and was nearly identical (99 ± 23% of control) on addition of the CA inhibitor.

The absence of an effect of CA on the alkalinization suggests that the transmembrane HCO_3^- fluxes generated by the cotransporter are sufficiently slow so that the reaction $HCO_3^- + H^+ \rightarrow CO_2 + H_2O$ (required to produce cell alkalinization) proceeds fast enough, even in the absence of CA. This is most likely the case, as changes in Müller cell pH_i, evoked by increases in P_{CO_2}, can occur at a rate of 0.36 pH units/min in the absence of CA (Newman, 1994). Similar results have been observed in leech glial cells (Rose and Deitmer, 1995a) in which the addition of a CA inhibitor has no effect on stimulus-evoked cell alkalinization.

Localization of Na^+/HCO_3^- cotransport with pH_i measurements

Results from previous electrophysiological studies of Na^+/HCO_3^- cotransport in Müller cells have demonstrated that cotransporter sites are localized preferentially to the cell endfoot (Newman and Astion, 1991; Newman, 1991). This finding implies that transmembrane HCO_3^- fluxes are largest at the endfoot and suggests that K^+-evoked intracellular alkalinization might be larger at the endfoot than in other cell regions. This prediction was tested by measuring the rates of K^+-evoked alkalinization in control cells and in cells that had lost their endfeet during the isolation procedure.

In a group of cells that lacked their endfeet and a large portion of their proximal processes, the rate of alkalinization evoked by increasing $[K^+]_o$ to 50 mM was equal to 0.030 ± 0.10 (15) pH units/min. In control cells from the same preparations, the alkalinization rate was 0.060 ± 0.019 (9). This finding, that cells with their endfeet intact have twice the alkalinization rate as cells without endfeet, is consistent with the presence of a greater density of Na^+/HCO_3^- cotransport sites at the endfoot.

Localization of cotransporter sites to the endfoot also was tested by simultaneously measuring K^+-induced alkalinization in the soma and endfoot regions of individual cells. If HCO_3^- flux is greater at the endfoot, this cell region may show a greater alkalinization rate than other regions.

This proved not to be the case. In all cells tested (n = 44), the alkalinization rate measured in the endfoot was nearly identical to the rate in the soma (Fig. 4). This result could be taken as evidence that cotransporter sites are not localized preferentially to the endfoot. Alternatively, K^+-evoked HCO_3^- fluxes could still be greater at the endfoot, but the rate of intracellular alkalinization too slow to establish a pH gradient within the cell. The rate at which acid/base equivalents diffuse within cells might be sufficiently rapid to prevent a measurable buildup of HCO_3^- at the endfoot. This seems likely, as HCO_3^- will diffuse from the endfoot to the soma, a distance of ~60 μm, in ~4.8 sec (calculated from the mean square diffusion distance and an effective diffusion coefficient, corrected for tortuosity (Nicholson and Phillips, 1981), of 3.75×10^{-6} cm^2 × sec^{-1}). This diffusion time is much shorter than the time it takes for K^+-induced alkalinization to develop.

Measurement of extracellular pH

The findings described above leave several questions unanswered, including the following: (1) does activation of the Na^+/HCO_3^- cotransporter lead to shifts in pH_o, (2) is the HCO_3^--independent component of intracellular alkalinization generated by a transmembrane acid/base flux, and (3) are cotransporters localized to the endfeet of Müller cells? These questions can be addressed by monitoring pH_o in the vicinity of isolated cells.

To measure pH_o, dissociated cells were placed on coverslips previously coated with the pH-indicator dye BCECF. The pH of the bath solution in the narrow space between cell and coverslip was monitored by ratio imaging of the dye. The pH_o in this narrow space is determined by a balance between cell transmembrane acid/base fluxes and diffusion of acid/base equivalents to the bulk bath solution. This imaging method can complement the widely used pH-sensitive microelectrode technique for measuring pH_o. Although pH electrodes have lower noise, pH_o imaging has the benefit of being able to determine pH values in many regions simultaneously. This is particularly advantageous when determining the localization of acid/base fluxes across the surface of a cell.

K^+-induced extracellular acidification

If the HCO_3^--dependent intracellular alkalinization evoked by raising $[K^+]_o$ is generated by modulation of the Na^+/HCO_3^- cotransporter, raising $[K^+]_o$ should also generate an extracellular acidification. This proved to be the case. Increasing $[K^+]_o$ from 2.5 to 50 mM evoked an extracellular acidification ranging from 0.01 to 0.05 pH units in amplitude (Fig. 5*B*, *"difference" trace*). The acidification was fully developed within seconds and reached plateau at a level that remained constant as long as $[K^+]_o$ remained high.

Changes in pH_o beneath cells reflect variations in bath pH as well as in cellular acid/base fluxes. This is a potential source of artifact when measuring pH_o, inasmuch as evoked pH_o changes are small and it is impossible to match the pH of different bath solutions perfectly. To minimize this source of artifact, pH_o changes beneath cells were always compared with the pH_o of the bulk solution. This was accomplished by subtracting pH_o values from regions of the coverslip in contact with the bulk solution (Fig. 5, *bath*) from regions lying beneath a cell (Fig. 5, *endfoot*). The resulting difference in pH_o measurements (Fig. 5*B*, *difference*) reflects transmembrane acid/base fluxes but not changes in the pH of the bath solution. pH_o measurements described in the experiments below were made using this "difference" correction.

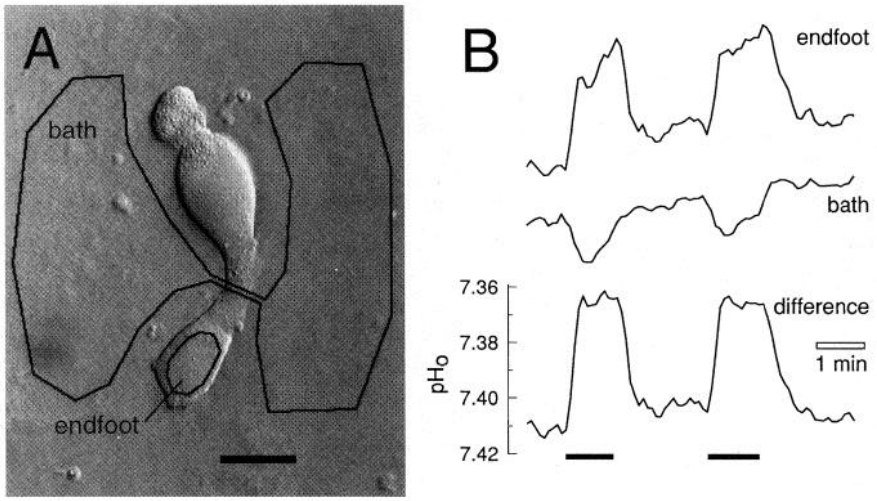

Figure 5. Measurement of K^+-evoked extracellular acidification beneath Müller cells. *A*, Nomarski micrograph of a dissociated Müller cell. Typical regions from which *endfoot* and *bath* pH_o are measured are indicated by *black outlines*. Scale bar, 20 μm. *B*, Records of pH_o variations evoked by $[K^+]_o$ increases. The corrected *endfoot* pH_o record (*difference plot*) is obtained by subtracting the *bath* record from the *endfoot* record. As indicated by the *bath* record, the pH of the 50 mM K^+ solution is slightly more alkaline than is the control solution. The *endfoot* and *bath* records have been offset vertically.

External carbonic anhydrase

Inhibition of CA enhanced the extracellular acidification evoked by raising $[K^+]_o$ to 50 mM. Addition of 2×10^{-5} M benzolamide, a potent CA inhibitor (Maren, 1967), increased the K^+-evoked acidification to 269 ± 141% (8) of the control increase (Fig. 6*A*). Benzolamide is charged at physiological pH and is poorly membrane permeant (Travis et al., 1963). It is ineffective in inhibiting intracellular CA in Müller cells (Newman, 1994). Thus, it is likely that benzolamide is acting on extracellular CA in its enhancement of the extracellular acidification. The CA inhibitor methazolamide, which can act on both intracellular and extracellular forms of the enzyme (Maren, 1967), enhanced the K^+-evoked extracellular acidification to the same degree as did benzolamide. All subsequent experiments monitoring pH_o were conducted in the presence of either benzolamide or methazolamide.

Na^+/HCO_3^- cotransport

If the K^+-induced extracellular acidification is generated solely by the cotransporter, the response should be abolished by removal of HCO_3^- from the bath solution and by addition of the cotransporter blocker DIDS. This proved to be the case.

Extracellular acidification evoked by raising $[K^+]_o$ to 50 mM was reduced to 7.0 ± 7.9% (6) of the control amplitude when the HCO_3^- Ringer's was replaced with HEPES Ringer's (Fig. 6*B*). Similarly, the addition of 0.5 mM DIDS reduced the K^+-evoked acidification to 7.8 ± 8.9% (5) of the control response (Fig. 6*C*).

Localization of Na^+/HCO_3^- cotransport with pH_o measurements

If cotransporter sites are preferentially localized to the endfoot of Müller cells, then K^+-induced extracellular acidification should be larger beneath the endfoot than beneath the soma. This proved to be true (Fig. 7*A*). The endfoot acidifications averaged 304 ± 119% (12) of the soma responses.

Regional variations in extracellular acidification also were evaluated by calculating difference ratio images. Images of BCECF fluorescence were obtained during control periods and during periods when the Na^+/HCO_3^- cotransporter was modulated by raising $[K^+]_o$ to 50 mM. The ratio images, calculated by dividing control by test images, reveal local changes in pH_o produced by cell stimulation.

Difference ratio images evoked by K^+ stimulation consistently showed that extracellular acidification was largest beneath the endfoot (Fig. 7*C*). The endfoot acidification was always greatest in the center of the endfoot and declined toward the edge of the cell, as expected if the acidification was being reduced by diffusion to the bulk solution.

Both temporal plots of pH_o changes (Fig. 7*A*) and difference ratio images of pH_o changes (Fig. 7*C*) confirm previous findings (Newman and Astion, 1991; Newman, 1991) showing that Na^+/HCO_3^- cotransporter sites are preferentially localized to the cell endfoot. One must be cautious when interpreting the pH_o results in a quantitative fashion, however, because several factors other than transporter density can influence the magnitude of extracellular acidification beneath a cell. Regional differences in pH_o could be because of variations in the space between cell and coverslip or the rate at which acid/base equivalents are cleared from beneath the cell. At a first approximation, however, these factors should not differ substantially in different cell regions.

DISCUSSION

Na^+/HCO_3^- cotransport

The results presented in this paper demonstrate that the Na^+/HCO_3^- cotransport system of salamander Müller cells modulates intracellular and extracellular pH in response to changes in $[K^+]_o$. Increasing $[K^+]_o$ results in an intracellular alkalinization and in an extracellular acidification. The extracellular acidification seems to be generated exclusively by the cotransport system, whereas a large fraction (but not all) of the intracellular alkalinization is generated by the cotransporter.

Previous electrophysiological findings demonstrated that amphibian Müller cells possess a Na^+/HCO_3^- cotransporter (Newman and Astion, 1991; Newman, 1991). In these earlier studies, cotransporter currents were recorded using the whole-cell voltage-clamp technique. The currents were HCO_3^-- and Na^+-dependent and were inhibited by DIDS, 4,4′-dinitrostilbene-2,2′-disulphonic acid (DNDS), and harmaline. The present results confirm the presence of the cotransporter in Müller cells. The observed K^+-evoked pH changes are generated by the cotransporter, inasmuch as they are HCO_3^--dependent and DIDS-sensitive.

Na^+/HCO_3^- cotransport activity is present in other glial cells, including astrocytes in gliotic rat hippocampal slices (Grichtchenko and Chesler, 1994a,b), cultured mammalian astrocytes (Boyarsky et al., 1993; Brookes and Turner, 1994; Brune et al., 1994; O'Connor et al., 1994; Shrode and Putnam, 1994) and oligodendrocytes (Kettenmann and Schlue, 1988), glial cells of the amphibian optic nerve (Astion and Orkand, 1988), and neuropil

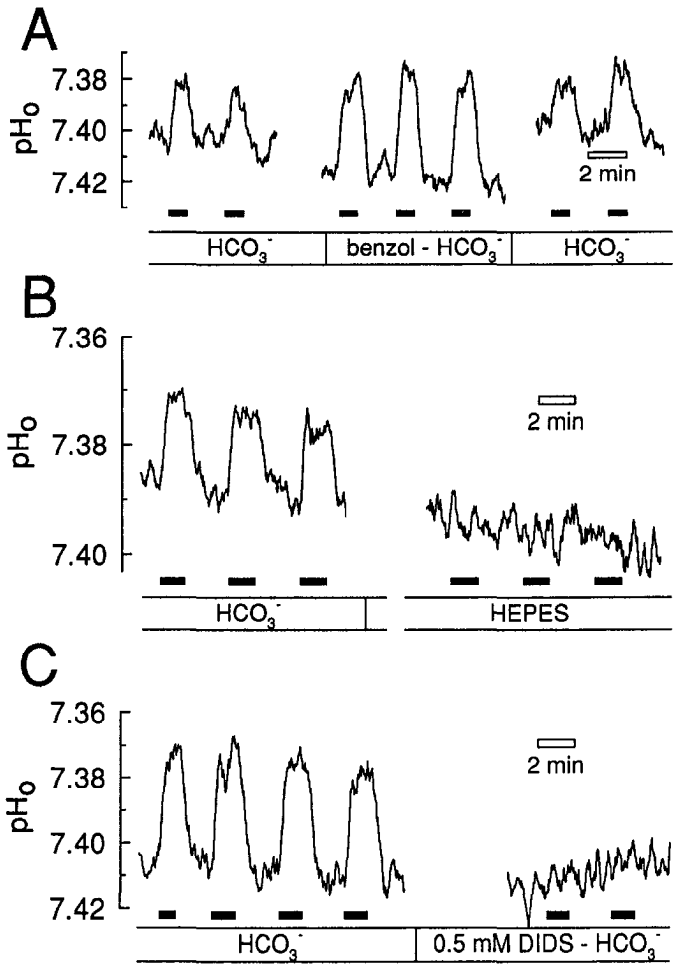

Figure 6. Potassium-evoked extracellular acidification. *A*, Addition of 2×10^{-5} M benzolamide (*benzol*), a CA inhibitor, increases the amplitude of the acidification in this example to 199% of control. When benzolamide is removed, the acidification returns to control amplitude. The shift in baseline pH_o during benzolamide application reflects drift in the measurement of pH and is not caused by benzolamide. pH_o is measured beneath the endfoot. Gaps in the record before and after benzolamide are 2.6 and 10.7 min in length. *B*, Substitution of HEPES for HCO_3^- Ringer's diminishes the K^+-evoked extracellular acidification to near zero. pH_o is measured beneath the endfoot. There is a 28.7 min gap in the record. *C*, Addition of 0.5 mM DIDS diminishes the acidification to near zero. pH_o is measured beneath the endfoot. There is a 6 min gap in the record.

glia of the leech (Deitmer and Schlue, 1989; Deitmer and Szatkowski, 1990; Munsch and Deitmer, 1994).

Extracellular acidification

The present results lend support to previous studies which have shown that glial cells contribute to pH_o changes in the CNS. In the enucleated rat optic nerve, which contains only glial cells, increased $[K^+]_o$ generates an extracellular acidification (Ransom et al., 1988). In the gliotic rat hippocampal slice, where few neurons are present, elevation of $[K^+]_o$ results in extracellular acidification as well (Grichtchenko and Chesler, 1994a,b). The acidification is Na^+- and HCO_3^--dependent, suggesting that it is generated by activation of a glial Na^+/HCO_3^- cotransporter. In addition, dissociated amphibian Müller cells, when stimulated with glutamate, generate an extracellular alkalinization arising from a glutamate uptake carrier that transports either OH or HCO_3^- out of cells as glutamate is transported in (Bouvier et al., 1992).

Other studies have also linked extracellular acidification to glial cells. In developmental studies of the rat optic nerve (Ransom et al., 1988) and spinal cord (Sykova et al., 1992a,b), increases in the amplitude of stimulus-evoked extracellular acidification parallel the proliferation and maturation of glial cells. In the spinal cord, a rapid extracellular acidification seems to be generated by a 4-acetamido-4′-isothiocyanato-stilbene-2,2′-disulfonic acid (SITS)-sensitive Na^+/HCO_3^- cotransport system (Sykova and Svoboda, 1990; Sykova et al., 1992b). In the neonatal rat spinal cord, x-irradiation leads to the disruption of normal glial development and to the loss of stimulus-evoked extracellular acidification (Sykova et al., 1992a). In the rat cortex *in vivo*, electrical stimulation results in glial cell alkalinization, which is correlated with cell depolarization (Chesler and Kraig, 1989). A DIDS-sensitive, stimulus-evoked extracellular acidification, generated by a Na^+/HCO_3^- cotransporter, also is observed in neuropil glial cells of the leech segmental ganglion (Rose and Deitmer, 1994, 1995a,b).

In the present experiments, elevated $[K^+]_o$ resulted in an acidification ranging from 0.01 to 0.05 pH units in amplitude. Because conditions differ markedly between the *in vitro* preparation used here and *in vivo* conditions, it is difficult to estimate the magnitude of a Müller cell acidification in the intact retina. On one hand, $[K^+]_o$ increases observed *in vivo* are much smaller than those used here (~0.5 mM vs 50 mM). On the other hand, clearance of the acidification will be less efficient *in vivo*, where cells are packed close together, than in the experimental preparation, where the acidification is rapidly cleared to the bulk solution by diffusion.

An estimate of the magnitude of a Müller cell-generated acidification *in vivo* can be made, however. A $[K^+]_o$ increase of 0.5 mM will generate a driving force for HCO_3^- influx ~19 times smaller that that generated by a 50 mM increase. If one assumes that diffusional clearance of the acidification occurs at one-tenth the rate and that the intercellular spacing is half of its value *in vitro*, then a 0.5 mM $[K^+]_o$ increase will generate an acidification of approximately the same amplitude as observed in this study.

Localization of cotransporter to endfoot

pH measurements confirm that Na^+/HCO_3^- cotransporter sites are localized preferentially to the endfoot in salamander Müller cells. In earlier voltage-clamp studies, cotransporter currents recorded at the endfoot were 6.5-fold greater than those recorded at the soma (Newman and Astion, 1991; Newman, 1991). In the present study, difference ratio images of K^+-evoked pH_o acidification (Fig. 7*C*) graphically demonstrate this localization, as do pH_i measurements of K^+-evoked alkalinization in cells with and without endfeet.

HCO_3^--independent intracellular alkalinization

Approximately 40% of the K^+-evoked intracellular alkalinization observed in the present study is HCO_3^--independent and DIDS-insensitive and is presumably generated by a mechanism other than Na^+/HCO_3^- cotransport. The alkalinization apparently is not attributable to transmembrane acid/base transport, as only 7–8% of the K^+-evoked extracellular acidification is HCO_3^--independent and DIDS-insensitive. A similar cotransporter-independent intracellular alkalinization has been observed in astrocytes in gliotic hippocampal slices (Grichtchenko and Chesler, 1994a). The alkalinization may be attributable to a K^+-evoked change in the metabolic state of the cell (Orkand et al., 1973; Salem et al., 1975), although the specific pathways that are involved remain unknown.

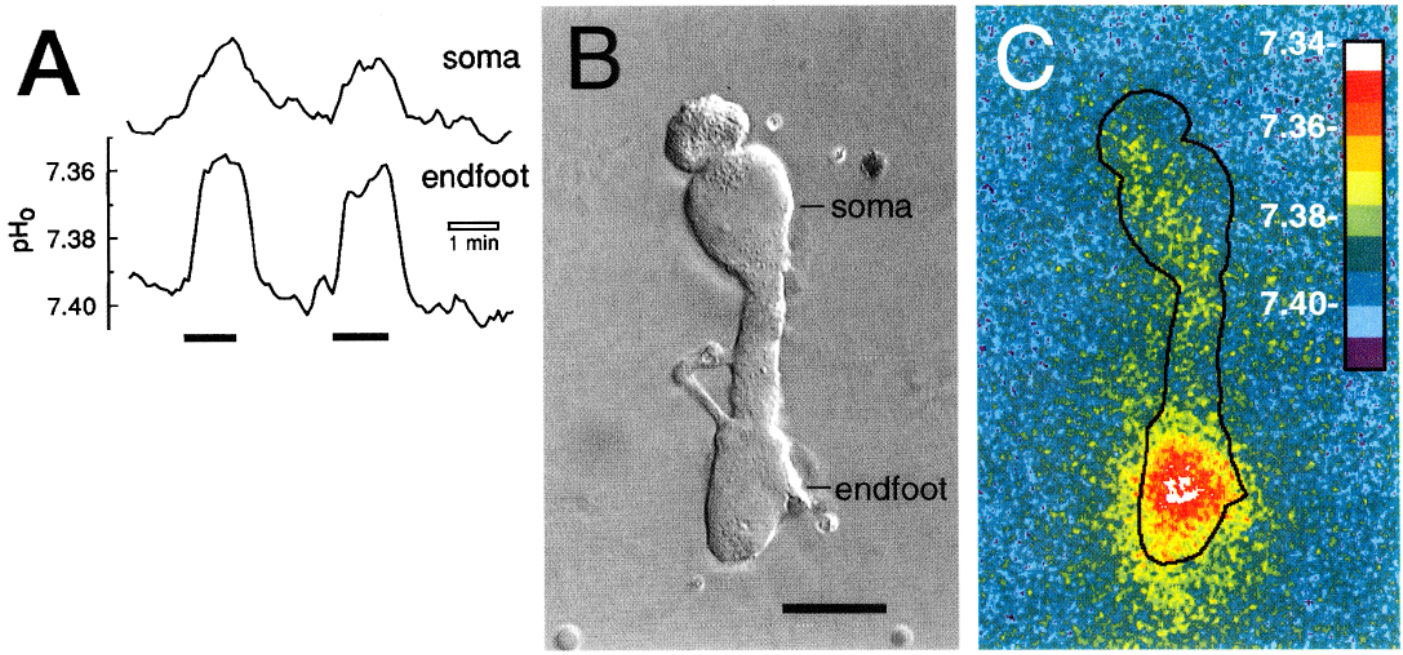

Figure 7. The amplitude of the K^+-evoked extracellular acidification is greater at the endfoot than at the soma. *A*, pH_o is recorded simultaneously beneath the *endfoot* and *soma* of a single cell in HCO_3^- Ringer's. The amplitude of the endfoot response in this example is 238% of the amplitude of the soma response. The soma record has been displaced vertically. *B*, Nomarski micrograph of a dissociated Müller cell. Scale bar, 20 μm. *C*, Difference ratio image of pH_o changes evoked by raising $[K^+]_o$ from 2.5 to 50 mM in HCO_3^- Ringer's. The image is of the same field as shown in *B*, with the position of the cell indicated by the *outline*. Increasing $[K^+]_o$ evokes an acidification that is largest beneath the endfoot (peak magnitude, 0.054 pH units) and small beneath other cell regions. pH_o is indicated by the color calibration bar in this pseudocolor image.

A HCO_3^--independent, K^+-evoked intracellular alkalinization attributable to a bafilomycin A_1-sensitive H^+-ATPase has been reported in cultured mammalian astrocytes (Pappas and Ransom, 1993). It is unlikely that a H^+-ATPase contributes significantly to the HCO_3^--independent intracellular alkalinization in Müller cells, however, because H^+-ATPase activation would generate an extracellular acidification.

External carbonic anhydrase

The experiments presented here provide evidence that salamander Müller cells possess extracellular CA activity. Addition of the extracellular CA inhibitor benzolamide at 2×10^{-5} M produces a 169% increase in the K^+-evoked extracellular acidification. It is unlikely that benzolamide is exerting its effect by inhibiting an internal component of CA; I have shown previously that benzolamide, at a higher concentration of 10^{-4} M, is ineffective in inhibiting intracellular CA (Newman, 1994).

It is possible that benzolamide is acting not on a native membrane-bound CA but on an enzyme contained in cell fragments adhering to dissociated cells. This is unlikely, as the dissociation procedure yields cells free of visible debris. It also is unlikely that intracellular CA is leaking out from dissociated cells; these cells maintain their integrity for many hours, as judged by electrophysiological criteria.

Numerous studies have demonstrated the importance of extracellular CA in reducing activity-dependent pH_o variations in the CNS. The addition of CA inhibitors results in enhancement of these pH_o variations (Borgula et al., 1989; Sykova and Svoboda, 1990; Chen and Chesler, 1992a; Grichtchenko and Chesler, 1994b; Rose and Deitmer, 1995a) and can modulate neuronal activity (Taira et al., 1993; Gottfried and Chesler, 1994). The results presented here demonstrate that Müller cells contribute to extracellular CA activity in the retina. This extracellular CA may help to regulate pH_o variations in the retina; previous studies have demonstrated that retinal, light-evoked pH_o transients are enhanced by the addition of CA inhibitors (Borgula et al., 1989; Oakley and Wen, 1989).

CA modulates pH_o variations because it catalyzes the reaction

$$CO_2 + H_2O \overset{CA}{\longleftrightarrow} H_2CO_3 \leftrightarrow H^+ + HCO_3^-,$$

which is the basis of pH_o buffering in the CNS (Chesler, 1990). The effective buffering power of the CO_2/HCO_3^- system for rapid changes in pH_o is substantially greater when CA is present. It is not clear, however, whether modulation of the CO_2/HCO_3^- buffer system accounts for the benzolamide enhancement of the extracellular acidification observed in the present study. Activation of the Na^+/HCO_3^- cotransporter is thought to lead to an influx of HCO_3^- into Müller cells and to a reduction in $[HCO_3^-]_o$. This decrease in $[HCO_3^-]_o$ generates an extracellular acidification that should be reduced, rather than increased, by the action of a CA inhibitor (Grichtchenko and Chesler, 1994a,b). Elucidation of the mechanism by which benzolamide enhances the K^+-evoked extracellular acidification awaits additional study.

Significance of extracellular acidification

Neutralization of extracellular alkalinization

Neuronal activity often is associated with a transient extracellular alkalinization, which is generated by glutamatergic and GABAergic receptors (Chesler, 1990; Chesler and Kaila, 1992). Calcium channels at synaptic terminals are pH-dependent (Barnes and Bui, 1991; Barnes et al., 1993; Takahashi et al., 1993), and the extracellular alkalinization, by increasing Ca^{2+} conductance, leads to enhanced synaptic transmission (Balestrino and Somjen, 1988;

Barnes et al., 1993). The extracellular acidification generated by glial cells, demonstrated in this and other studies, may function to partially balance this fast alkalinization thus minimizing changes in synaptic efficacy. In a similar manner, acid efflux from glia could serve as a component of a negative feedback system, regulating neuronal activity (Ransom, 1992). As neuronal activity increases, raising $[K^+]_o$ and depolarizing glial cells, the acidification produced by the glial Na^+/HCO_3^- cotransporter will reduce the conductance of neuronal ion channels and depress neuronal excitability.

In the retina, light stimulation produces an extracellular alkalinization in the inner plexiform (synaptic) layer and in the photoreceptor layer (Borgula et al., 1989; Yamamoto et al., 1992). Modulation of the Müller cell Na^+/HCO_3^- cotransporter, generating an extracellular acidification, may help to counter this alkalinization.

Regulation of blood flow

In both the retina (Riva et al., 1991; Scheiner et al., 1994) and the brain (Roy and Sherrington, 1890; Fox and Raichle, 1984), increases in neuronal activity result in increased blood flow. I have proposed previously that glial cells mediate this homeostatic response by releasing acid equivalents onto blood vessels (Newman, 1991). (Vessels are pH-sensitive and dilate when pH_o acidifies; McCulloch et al., 1982.) The endfeet of both Müller cells and astrocytes terminate directly onto blood vessels in the CNS. The demonstration that increased $[K^+]_o$ results in an extracellular acidification and particularly that this acidification is preferentially localized to cell endfeet provides support for this hypothesis of glial cell regulation of blood flow.

REFERENCES

Astion ML, Orkand RK (1988) Electrogenic Na^+/HCO_3^- cotransport in neuroglia. Glia 1:355–357.

Balestrino M, Somjen GG (1988) Concentration of carbon dioxide, interstitial pH and synaptic transmission in hippocampal formation of the rat. J Physiol (Lond) 396:247–266.

Barnes S, Bui Q (1991) Modulation of calcium-activated chloride current via pH-induced changes of calcium channel properties in cone photoreceptors. J Neurosci 11:4015–4023.

Barnes S, Merchant V, Mahmud F (1993) Modulation of transmission gain by protons at the photoreceptor output synapse. Proc Natl Acad Sci USA 90:10081–10085.

Borgula GA, Karwoski CJ, Steinberg RH (1989) Light-evoked changes in extracellular pH in frog retina. Vision Res 29:1069–1077.

Boron WF, Boulpaep EL (1983) Intracellular pH regulation in the renal proximal tubule of the salamander. Basolateral HCO_3^- transport. J Gen Physiol 81:53–94.

Boron WF, Boulpaep EL (1989) The electrogenic Na/HCO_3 cotransporter. Kidney Int 36:392–402.

Bouvier M, Szatkowski M, Amato A, Attwell D (1992) The glial cell glutamate uptake carrier countertransports pH-changing anions. Nature 360:471–474.

Boyarsky G, Ransom B, Schlue W-R, Davis MBE, Boron WF (1993) Intracellular pH regulation in single cultured astrocytes from rat forebrain. Glia 8:241–248.

Brookes N, Turner RJ (1994) K^+-induced alkalinization in mouse cerebral astrocytes mediated by reversal of electrogenic Na^+-HCO_3^- cotransport. Am J Physiol 267:C1633–C1640.

Brune T, Fetzer S, Backus KH, Deitmer JW (1994) Evidence for electrogenic sodium-bicarbonate cotransport in cultured rat cerebellar astrocytes. Pflügers Arch 429:64–71.

Chen JCT, Chesler M (1992a) pH transients evoked by excitatory synaptic transmission are increased by inhibition of extracellular carbonic anhydrase. Proc Natl Acad Sci USA 89:7786–7790.

Chen JCT, Chesler M (1992b) Modulation of extracellular pH by glutamate and GABA in rat hippocampal slices. J Neurophysiol 67:29–36.

Chesler M (1990) The regulation and modulation of pH in the nervous system. Prog Neurobiol 34:401–427.

Chesler M, Kaila K (1992) Modulation of pH by neuronal activity. Trends Neurosci 15:396–402.

Chesler M, Kraig RP (1989) Intracellular pH transients of mammalian astrocytes. J Neurosci 9:2011–2019.

Deitmer JW, Schlue WR (1989) An inwardly directed electrogenic sodium-bicarbonate cotransport in leech glial cells. J Physiol (Lond) 411:179–194.

Deitmer JW, Szatkowski M (1990) Membrane potential dependence of intracellular pH regulation by identified glial cells in the leech central nervous system. J Physiol (Lond) 421:617–631.

Fox PT, Raichle ME (1984) Stimulus rate dependence of regional cerebral blood flow in human striate cortex, demonstrated by positron emission tomography. J Neurophysiol 51:1109–1120.

Gottfried JA, Chesler M (1994) Endogenous H^+ modulation of NMDA receptor-mediated EPSCs revealed by carbonic anhydrase inhibition in rat hippocampus. J Physiol (Lond) 478:373–378.

Grichtchenko II, Chesler M (1994a) Depolarization-induced alkalinization of astrocytes in gliotic hippocampal slices. Neuroscience 62:1071–1078.

Grichtchenko II, Chesler M (1994b) Depolarization-induced acid secretion in gliotic hippocampal slices. Neuroscience 62:1057–1070.

Harsanyi K, Mangel SC (1993) Modulation of cone to horizontal cell transmission by calcium and pH in the fish retina. Vis Neurosci 10:81–91.

Hughes BA, Adorante JS, Miller SS, Lin H (1989) Apical electrogenic $NaHCO_3$ cotransport. A mechanism for HCO_3 absorption across the retinal pigment epithelium. J Gen Physiol 94:125–150.

Jarolimek W, Misgeld U, Lux HD (1989) Activity dependent alkaline and acid transients in guinea pig hippocampal slices. Brain Res 505:225–232.

Kaila K, Paalasmaa P, Taira T, Voipio J (1992) pH transients due to monosynaptic activation of $GABA_A$ receptors in rat hippocampal slices. NeuroReport 3:105–108.

Kettenmann H, Schlue WR (1988) Intracellular pH regulation in cultured mouse oligodendrocytes. J Physiol (Lond) 406:147–162.

Kleinschmidt J (1994) Signal transmission at the photoreceptor synapse. Role of calcium ions and protons. Ann NY Acad Sci 468–470.

Klockner U, Isenberg G (1994) Calcium channel current of vascular smooth muscle cells: extracellular protons modulate gating and single channel conductance. J Gen Physiol 103:665–678.

Krafte DS, Kass RS (1988) Hydrogen ion modulation of Ca channel current in cardiac ventricular cells. J Gen Physiol 91:641–657.

Maren TH (1967) Carbonic anhydrase: chemistry, physiology, and inhibition. Physiol Rev 47:597–781.

McCulloch J, Edvinsson L, Watt P (1982) Comparison of the effects of potassium and pH on the calibre of cerebral veins and arteries. Pflügers Arch 393:95–98.

Munsch T, Deitmer JW (1994) Sodium-bicarbonate cotransport current in identified leech glial cells. J Physiol (Lond) 474:43–53.

Newman EA (1985) Membrane physiology of retinal glial (Müller) cells. J Neurosci 5:2225–2239.

Newman EA (1991) Sodium-bicarbonate cotransport in retinal Müller (glial) cells of the salamander. J Neurosci 11:3972–3983.

Newman EA (1994) A physiological measure of carbonic anhydrase in Müller cells. Glia 11:291–299.

Newman EA, Astion ML (1991) Localization and stoichiometry of electrogenic sodium-bicarbonate cotransport in retinal glial cells. Glia 4:424–428.

Nicholson C, Phillips JM (1981) Ion diffusion modified by tortuosity and volume fraction in the extracellular microenvironment of the rat cerebellum. J Physiol 321:225–257.

Oakley BI, Wen R (1989) Extracellular pH in the isolated retina of the toad in darkness and during illumination. J Physiol (Lond) 419:353–378.

O'Connor ER, Sontheimer H, Ransom BR (1994) Rat hippocampal astrocytes exhibit electrogenic sodium-bicarbonate cotransport. J Neurophysiol 72:2580–2589.

Orkand PM, Bracho H, Orkand RK (1973) Glial metabolism: alteration by potassium levels comparable to those during neural activity. Brain Res 55:467–471.

Pappas CA, Ransom BR (1993) A depolarization-stimulated, bafilomycin-inhibitable H^+-pump in hippocampal astrocytes. Glia 9:280–291.

Prod'hom B, Pietrobon D, Hess P (1987) Direct measurement of proton transfer rates to a group controlling the dihydropyridine-sensitive Ca^{2+} channel. Nature 329:243–246.

Ransom BR (1992) Glial modulation of neural excitability mediated by extracellular pH: a hypothesis. Prog Brain Res 94:37–46.

Ransom BR, Carlini WG, Connors BW (1988) Brain extracellular space: developmental studies in rat optic nerve. Ann NY Acad Sci 481:87–105.

Riva CE, Harino S, Shonat RD, Petrig BL (1991) Flicker evoked increase in optic nerve head blood flow in anesthetized cats. Neurosci Lett 128:291–296.

Rose CR, Deitmer JW (1994) Evidence that glial cells modulate extracellular pH transients induced by neuronal activity in the leech central nervous system. J Physiol 481:1–5.

Rose CR, Deitmer JW (1995a) Stimulus-evoked changes of extra- and intracellular pH in the leech central nervous system. II. Mechanisms and maintenance of pH homeostasis. J Neurophysiol 73:132–140.

Rose CR, Deitmer JW (1995b) Stimulus-evoked changes of extra- and intracellular pH in the leech central nervous system. I. Bicarbonate dependence. J Neurophysiol 73:125–131.

Roy CS, Sherrington CS (1890) On the regulation of the blood-supply of the brain. J Physiol (Lond) 11:85–108.

Salem RD, Hammerschlag R, Bracho H, Orkand RK (1975) Influence of potassium ions on accumulation and metabolism of [^{14}C]glucose by glial cells. Brain Res 86:499–503.

Scheiner AJ, Riva CE, Kazahaya K, Petrig BL (1994) Effect of flicker on macular blood flow assessed by the blue field simulation technique. Invest Ophthalmol Vision Sci 35:3436–3441.

Shrode LD, Putnam RW (1994) Intracellular pH regulation in primary rat astrocytes and C6 glioma cells. Glia 12:196–210.

Soleimani M, Grassl SM, Aronson PS (1987) Stoichiometry of Na^-–HCO_3^- cotransport in basolateral membrane vesicles isolated from rabbit renal cortex. J Clin Invest 79:1276–1280.

Sykova E, Jendelova P, Simonova Z, Chvatal A (1992a) K^+ and pH homeostasis in the developing rat spinal cord is impaired by early postnatal X-irradiation. Brain Res 594:19–30.

Sykova E, Jendelova P, Svoboda J, Chvatal A (1992b) Extracellular K^+, pH, and volume changes in spinal cord of adult rats and during postnatal development. Can J Physiol Pharmacol 70:S301–S309.

Sykova E, Svoboda J (1990) Extracellular alkaline-acid-alkaline transients in the rat spinal cord evoked by peripheral stimulation. Brain Res 512:181–189.

Taira T, Smirnov S, Voipio J, Kaila K (1993) Intrinsic proton modulation of excitatory transmission in rat hippocampal slices. NeuroReport 4:93–96.

Takahashi K, Dixon DB, Copenhagen DR (1993) Modulation of a sustained calcium current by intracellular pH in horizontal cells of fish retina. J Gen Physiol 101:695–714.

Tang C-M, Dichter M, Morad M (1990) Modulation of the *N*-methyl-D-aspartate channel by extracellular H^+. Proc Natl Acad Sci USA 87:6445–6449.

Travis DM, Wiley C, Nechay BR, Maren TH (1963) Selective renal carbonic anhydrase inhibition without respiratory effect: pharmacology of 2-benzenesulfonamido-1,3,1-thiadiazole-5-sulfonamide (CL 11,366). J Pharmacol Exp Ther 143:383–394.

Traynelis SF, Cull-Candy SG (1990) Proton inhibition of *N*-methyl-D-aspartate receptors in cerebellar neurons. Nature 345:347–350.

Voipio J, Kaila K (1993) Interstitial P_{CO_2} and pH in rat hippocampal slices measured by means of a novel fast CO_2/H^+-sensitive microelectrode based on a PVC-gelled membrane. Pflügers Arch 423:193–201.

Yamamoto F, Borgula GA, Steinberg RH (1992) Effects of light and darkness on pH outside rod photoreceptors in the cat retina. Exp Eye Res 54:685–697.